

LEVEL

12
D.S.

ADA 072818

14

RADC-TR-79-17

In-House Report

January 1979

11



6

**ANALYSIS OF THE RESPONSE
OF AN RF INTRUDER PROTECTION
SYSTEM**

10

**J. Leon Poirier
Martin Kushner**

12 *22p.*

**DDC
RECEIVED
AUG 17 1979
C**

16 *4.00*

17 *15*

APPROVED FOR PUBLIC RELEASE; DISTRIBUTION UNLIMITED

DDC FILE COPY

**ROME AIR DEVELOPMENT CENTER
Air Force Systems Command
Griffis Air Force Base, New York 13441**

309 050

79 08 16 007

LB

This report has been reviewed by the RADC Information Office (OI) and is releasable to the National Technical Service (NTIS). At NTIS it will be releasable to the general public, including foreign nations.

RADC-TR-79-17 has been reviewed and is approved for publication.

APPROVED:



PHILIPP BLACKSMITH
Chief, EM Systems Concepts Branch

APPROVED:



ALLAN C. SCHELL
Chief, Electromagnetic Sciences Division

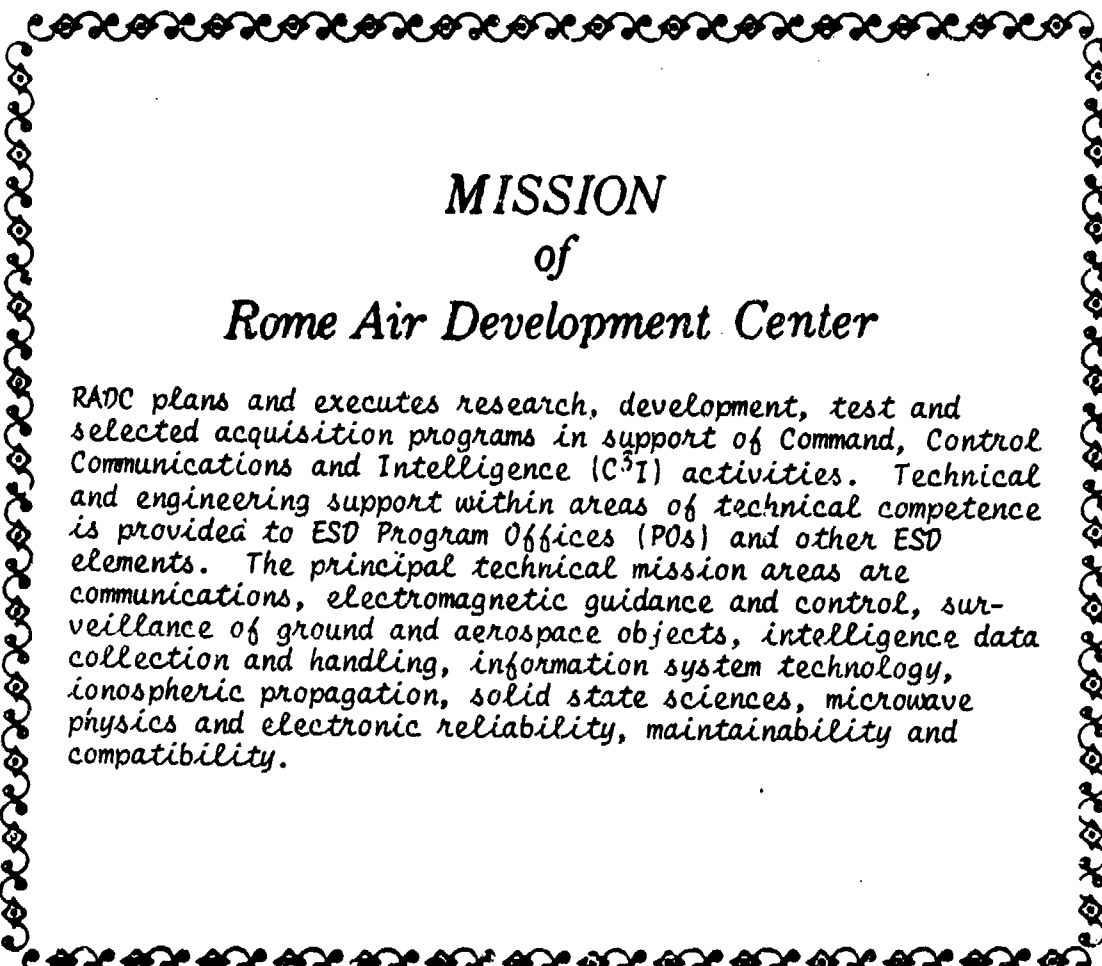
FOR THE COMMANDER:



JOHN P. HUSS
Acting Chief, Plans Office

If your address has changed or if you wish to be removed from the RADC mailing list, or if the addressee is no longer employed by your organization, please notify RADC (EEC) Hanscom AFB MA 01731. This will assist us in maintaining a current mailing list.

Do not return this copy. Retain or destroy.



MISSION
of
Rome Air Development Center

RADC plans and executes research, development, test and selected acquisition programs in support of Command, Control Communications and Intelligence (C³I) activities. Technical and engineering support within areas of technical competence is provided to ESD Program Offices (POs) and other ESD elements. The principal technical mission areas are communications, electromagnetic guidance and control, surveillance of ground and aerospace objects, intelligence data collection and handling, information system technology, ionospheric propagation, solid state sciences, microwave physics and electronic reliability, maintainability and compatibility.

Printed by
United States Air Force
Hanscom AFB, Mass. 01731

Unclassified

SECURITY CLASSIFICATION OF THIS PAGE (When Data Entered)

REPORT DOCUMENTATION PAGE		READ INSTRUCTIONS BEFORE COMPLETING FORM
1. REPORT NUMBER RADC-TR-79-17	2. GOVT ACCESSION NO.	3. RECIPIENT'S CATALOG NUMBER
4. TITLE (and Subtitle) ANALYSIS OF THE RESPONSE OF AN RF INTRUDER PROTECTION SYSTEM	5. TYPE OF REPORT & PERIOD COVERED In-House Report	
	6. PERFORMING ORG. REPORT NUMBER	
7. AUTHOR(s) J. Leon Poirier Martin Kushner	8. CONTRACT OR GRANT NUMBER(s)	
9. PERFORMING ORGANIZATION NAME AND ADDRESS Deputy for Electronic Technology (RADC/EEC) Hanscom AFB Massachusetts 01731	10. PROGRAM ELEMENT, PROJECT, TASK AREA & WORK UNIT NUMBERS 62702F 46001501	
11. CONTROLLING OFFICE NAME AND ADDRESS Deputy for Electronic Technology (RADC/EEC) Hanscom AFB Massachusetts 01731	12. REPORT DATE January 1979	
	13. NUMBER OF PAGES 20	
14. MONITORING AGENCY NAME & ADDRESS (if different from Controlling Office)	15. SECURITY CLASS. (of this report) Unclassified	
	15a. DECLASSIFICATION/DOWNGRADING SCHEDULE	
16. DISTRIBUTION STATEMENT (of this Report) Approved for public release; distribution unlimited.		
17. DISTRIBUTION STATEMENT (of the abstract entered in Block 20, if different from Report)		
18. SUPPLEMENTARY NOTES		
19. KEY WORDS (Continue on reverse side if necessary and identify by block number) Intrusion detection Aircraft protection Leaky coaxial cables Surveillance		
20. ABSTRACT (Continue on reverse side if necessary and identify by block number) A phenomenological theory has been developed to describe the variation in received signal power observed when an intruder penetrated the detection zone of an RF individual resource protection sensor. The sensor consisted of a loop of leaky coaxial cable which acted as a distributed transmitting antenna encircling the resource. A centrally located monopole served as a receiving antenna. The theory assumes that the principal effect of an intruder is to scatter some energy out of the leaky cable field. The variation in		

DD FORM 1473 EDITION OF 1 NOV 65 IS OBSOLETE
1 JAN 73

Unclassified

SECURITY CLASSIFICATION OF THIS PAGE (When Data Entered)

Unclassified

SECURITY CLASSIFICATION OF THIS PAGE(When Data Entered)

20. Abstract (Continued)

received power was produced as a result of the interference between the scattered field and the quiescent field present in the absence of an intruder. The phase and amplitude of the scattered field changed with the intruder's position, giving rise to a characteristic interference pattern related to system and environment properties. Good agreement was obtained between the predicted and measured response of several system configurations.

Unclassified

SECURITY CLASSIFICATION OF THIS PAGE(When Data Entered)

Accession For	
NTIS Grant	<input checked="" type="checkbox"/>
DDC TAB	<input type="checkbox"/>
Unannounced	<input type="checkbox"/>
Justification	<input type="checkbox"/>
By _____	
Distribution _____	
Availability _____	
Dist	_____
A	_____

Contents

1. INTRODUCTION	5
2. VARIATION IN RECEIVED POWER	8
2.1 Response to an Intruder for a Circular Loop	9
2.2 Response to an Intruder for a Square Loop	13
3. DISCUSSION	17
4. CONCLUSION	19
REFERENCES	20

Illustrations

1. Intrusion Sensor Layout	6
2. Attenuation Factors for Several Leaky Coaxial Cables	7
3. Coupling Loss for Three Leaky Coaxial Cables	7
4. Received Power Variation	11
5. Received Power Variation. $\alpha_1 \ll \alpha_2$	11
6. Received Power Variation for Large Intruder Signal	12
7. Received Power Variation for Circumferential Walk	12
8. Sketch of Square Loop Configuration	14
9. Plot of Local Phase Constant versus Intruder Location	15

Illustrations

10. Received Power Variation for Square Loop. $\alpha_1 \approx \alpha_2$	16
11. Received Power Variation for Square Loop for Small Intruder Signal	16
12. Measured Received Power Variation for Square Loop	17
13. Variation in Signal Power for Circular Loop of Radial Cable	18

Analysis of the Response of an RF Intruder Protection System

1. INTRODUCTION

Leaky coaxial cables have been used extensively in communications applications^{1, 2} and more recently in intrusion sensors.³ One such sensor^{4, 5} uses a length of leaky coaxial cable, encircling the resource to be protected, as a distributed transmitting antenna. A receiving antenna is located near the center of the loop. When an intruder approaches the cable, the field is disturbed and the received signal changes. This change is processed and if sufficiently large, a detection declared. It is this variation in received signal strength produced by an intruder in the vicinity of the leaky cable that is analyzed here.

(Received for publication 9 February 1979)

1. Delogne, P. (1976) Basic mechanisms of tunnel propagation, Radio Sci. 11:295-303.
2. De Keyser, R., Delogne, P., Deryck, L., and Liegeois, R. (1978) Comparative analysis of leaky cable techniques for mine communications, Proc. Workshop on Electromagnetic Guided Waves in Mine Environments.
3. Harman, R. K., Mackay, N.A.M. (1976) GUIDAR: An intrusion detection system for perimeter protection, Proc. 1976 Carnahan Conference on Crime Countermeasures, University of Kentucky, Lexington, Ky.
4. Poirier, J.L., Karas, N.V., Antonucci, J.A., and Szczytko, M. (1977) VHF Intrusion Detection: A Technique for Parked Aircraft, RADC-TR-77-384, AD A051144.
5. Karas, N.V., Poirier, J.L., Antonucci, J.A., and Szczytko, M. (1978) A VHF Intrusion Detection Technique for Isolated Resources, RADC-TR-78-177, AD A060791.

The elements of a basic system are shown in Figure 1. One end of the leaky coaxial cable is connected to a low-power transmitter; the other end is terminated in a matched load. The receiving element is a monopole antenna. The received signal is processed by appropriate filters and thresholding circuits in order to maximize the detection sensitivity for human frame motion.

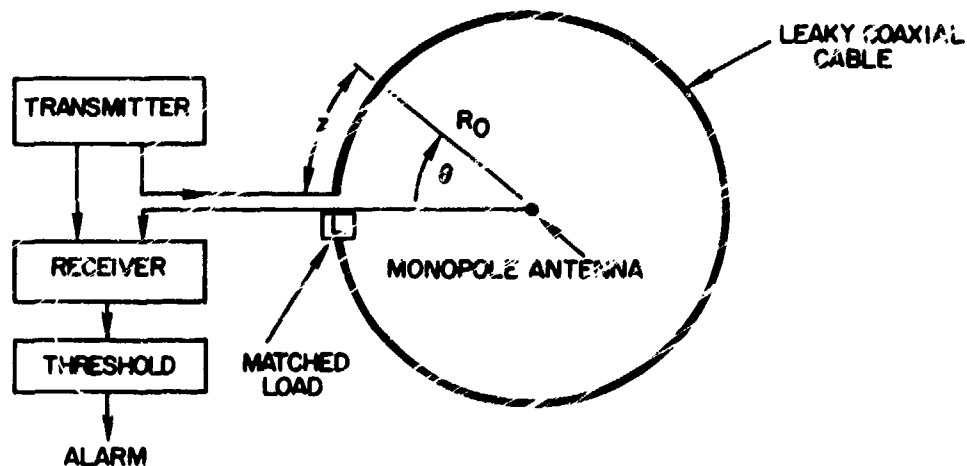


Figure 1. Intrusion Sensor Layout

A leaky coaxial cable is characterized by its attenuation and coupling loss. The attenuation factor is dependent on construction of the cable, the properties of the medium near, or in which the cable is placed, and the operating frequency. Typical values are shown in Figure 2 for several^{6, 7} cable types. As shown, the attenuation factor for RX4-3 is affected more by its environment than the attenuation factor for RX4-1. This is due to larger holes in the outer conductor of the former.

Coupling loss is defined as the ratio of signal power received by a dipole, located near a long-leaky cable, to the cable's input power. The specified antenna spacing is 20 ft., but since the fields associated with leaky cables exhibit a significant structure, manufacturers average the coupling loss for a range around 20 feet. For a particular cable type, the larger the holes the smaller the coupling loss. Typical values for some cables are shown in Figure 3.

6. Bulletin 1058A, Radlax Slotted Coaxial Cable, Andrew Corp., Orland Park, Ill.

7. Technical Memo 49, Revision No. 1, Times Wire and Cable Co., Wallingford, Connecticut.

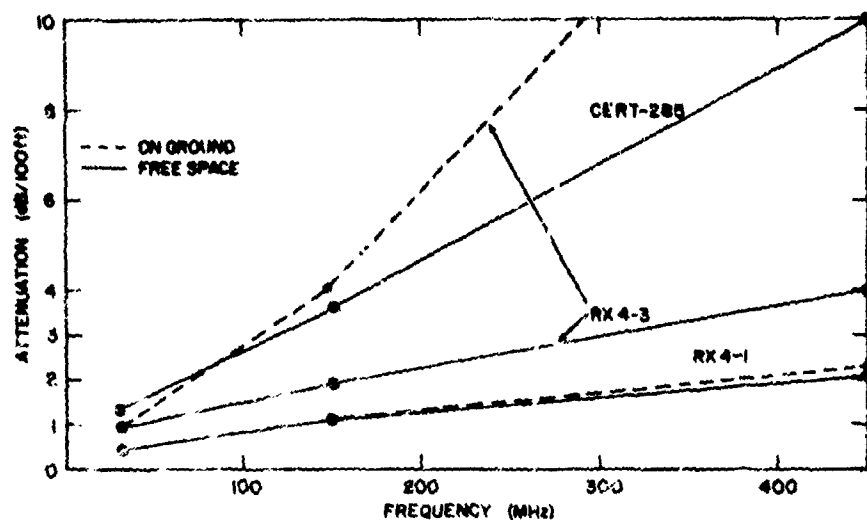


Figure 2. Attenuation Factors for Several Leaky Coaxial Cables

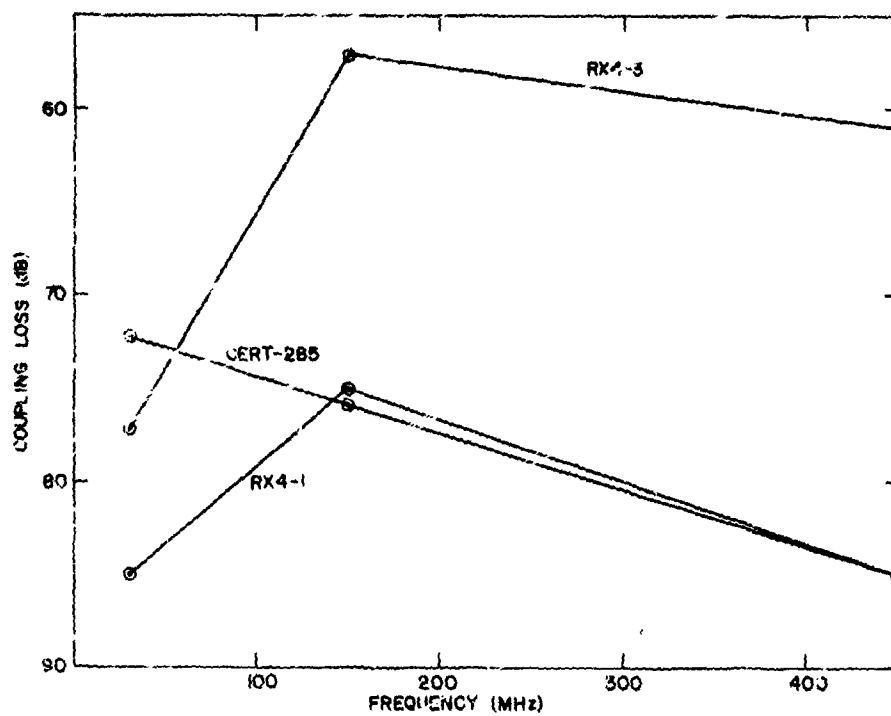


Figure 3. Coupling Loss for Three Leaky Coaxial Cables

For the purposes of this analysis, the field outside the leaky coaxial cable will be represented as

$$v = v_0 \left\{ e^{(-\alpha_1 + j\beta_1)z} + C_2 e^{(-\alpha_2 + j\beta_2)z} \right\} \quad (1)$$

where z is the distance from the cable input.

The first term is the contribution to the total field produced by the energy propagating inside the cable and leaking to the outside in the neighborhood of point z ; the second term describes the surface wave field set up by the internal energy leaking out along the cable. The surface wave field is continually refreshed because holes exist along the entire length cable. The constants v_0 and C_2 depend on the properties of the cable and medium. The attenuation and phase constants, α and β , also depend on the medium. The degree to which α_1 is affected depends on the coupling loss of the cable; that is, cables with high coupling loss are less affected by their environment (Figure 2). In contrast to α_1 , the attenuation constant α_2 is very sensitive to the nature of the environment. The phase constants are

$$\beta_1 = \frac{2\pi f}{v_1} \quad \text{and} \quad \beta_2 = \frac{2\pi f}{v_2}$$

where f is the operating frequency and v_1 and v_2 , the propagation velocities of the inner and surface waves, respectively.

If α_1 and α_2 are not too different, the intensity of the total external field will vary along the cable due to interaction of the two waves. In general, they propagate at different velocities and so their relative phase advances along the cable. However, it is often observed that α_2 is much larger than α_1 , whereupon this interaction soon dies away.

In the next sections, Eq. (1) will be used to estimate the intensity of the signal at the central monopole of the system (Figure 1) and its variation when an intruder enters the zone of detection.

2. VARIATION IN RECEIVED POWER

In the absence of an intruder, the voltage at the receiving antenna terminals is the result of many contributions from all parts of the transmitting cable. For a particular set of conditions, this voltage will be represented as

$$V = Be^{i\phi} \quad (2)$$

where the effective amplitude B and phase ϕ can be related to the operating frequency and the system parameters.

2.1 Response to an Intruder for a Circular Loop

In practice, an intruder would approach the leaky coaxial sensor along a radial and enter the zone of detection of the system only when he is within the immediate vicinity of the cable. In this analysis, the simulated intruder path will be along the cable in order that the detection sensitivity around the circumference of the leaky cable sensor can be estimated.

The variation in output power produced by an intruder is calculated by assuming that the effect of an intruder near the leaky coaxial is to scatter some of the field, described by Eq. (1), in which he is immersed. The voltage developed at the antenna as a result of the scattered field can be expressed as

$$V_I = PA v_o \left\{ e^{(-\alpha_1 + j\beta_1)z} + C_2 e^{(-\alpha_2 + j\beta_2)z} \right\} \quad (3)$$

where the constant A is the amplitude of the voltage at the antenna terminals produced by the scattered field; P accounts for propagation effects. Thus the total voltage at the antenna terminals is the sum of V and V_I and represented by

$$V_T = V + V_I \quad (4)$$

As an intruder walks around the loop, the phase and amplitude of the scattered voltage change. The variation in signal intensity thus produced as the quiescent voltage V and V_I interfere is obtained by multiplying V_T by its complex conjugate V_T^* . Thus

$$V_T V_T^* = VV^* + 2 \operatorname{Re} VV_I^* + V_I V_I^* \quad (5)$$

where Re signifies the real part of VV_I^* .

From Eqs. (2) and (3), the received power is found to be proportional to

$$\begin{aligned} V_T V_T^* = & B^2 + 2|v_o| |P| AB \left[e^{-\alpha_1 z} \cos(\phi - \beta_1 z - \delta) \right. \\ & \left. + C_2 e^{-\alpha_2 z} \cos(\phi - \beta_2 z - \delta) \right] + |v_o|^2 |P|^2 A^2 \\ & \left[e^{-2\alpha_1 z} + 2C_2 e^{(-\alpha_1 - \alpha_2)z} \cos(\beta_2 - \beta_1)z + C_2^2 e^{-2\alpha_2 z} \right] \quad (6) \end{aligned}$$

where δ is the phase angle associated with $v_o^* P^*$. The first term is proportional to the quiescent power, the second to the cross power, and the third to the intruder power.

The variation, in dB, relative to the quiescent level, can be expressed as

$$P_Q = 10 \log \left(\frac{V_T V_T^*}{V V^*} \right) . \quad (7)$$

Equation (7) was evaluated for a number of cases to determine the sensitivity of the system response to various parameters. The curve shown in Figure 4 gives the response for $\alpha_1 = 0.0074$ neper/m and $\alpha_2 = 0.0151$ neper/m. The modulation envelope clearly shows the effect of the surface wave with a higher propagation velocity than the energy propagation inside the cable. The gradual reduction in the over-all amplitude of the response is caused by the attenuation of the leaky coaxial cable. The gradual reduction in the amplitude of the surface wave-inner wave interaction arises because the attenuation of the surface wave is greater than that of the inner wave. The value of C_2 , together with the relative attenuation rates, determines the visibility of this interaction.

The effect of increasing the attenuation factor α_2 of the surface wave is demonstrated in Figure 5. Here it is seen that the over-all interaction dies out about halfway around the cable. Beyond that point, there is only a gradual reduction in response due to α_1 . This implies that the energy at any point along the cable is due primarily to the energy leaking out in that region, with very little coming from the surface wave.

The effect of changing the relative size of the intruder signal is demonstrated in Figure 6. Here the intruder voltage was made 50 percent greater than the quiescent voltage. The amplitude of the response is somewhat greater for small azimuth angles although the visibility of the interference is impaired. As the magnitude of the intruder voltage decreases with position, it becomes more nearly equal to the quiescent voltage and the quality of the interference increases to a maximum. Further along the cable, the intruder voltage becomes smaller than the quiescent voltage, and the response continually decreases until the end of the cable.

A recording obtained when an intruder walked around a 500-ft cable is shown in Figure 7. The rapid oscillations are produced as a result of the interference between the scattered intruder signal and the quiescent voltage. The slower modulation caused by the surface wave is evident as also the gradual reduction in response due to attenuation. The fine structure observable at the peak of each cycle is caused by the motion of the intruder's arms and legs which modulates his

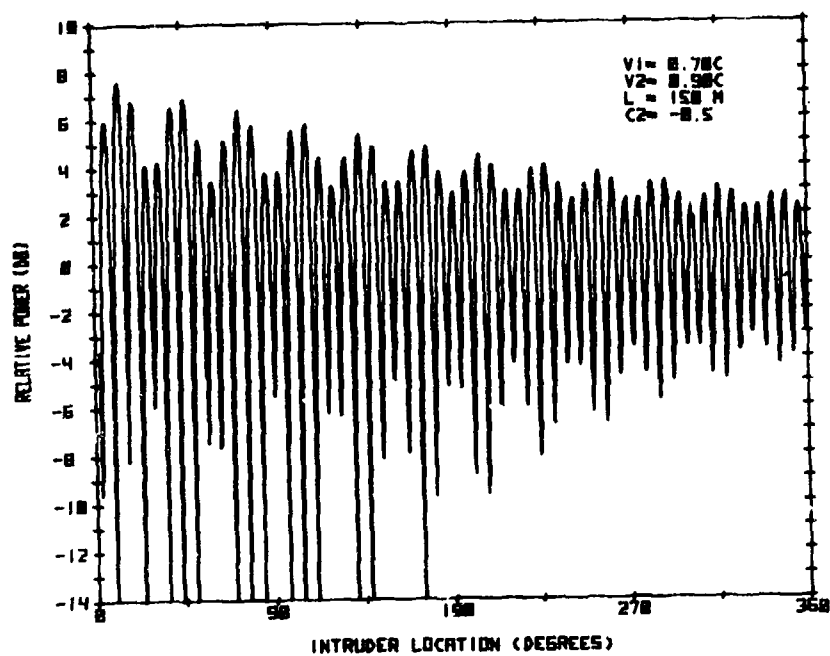


Figure 4. Received Power Variation. $|V| = |V_I|$, $\alpha_1 = 7.5 \times 10^{-3}$ neper/m, and $\alpha_2 = 1.51 \times 10^{-2}$ neper/m

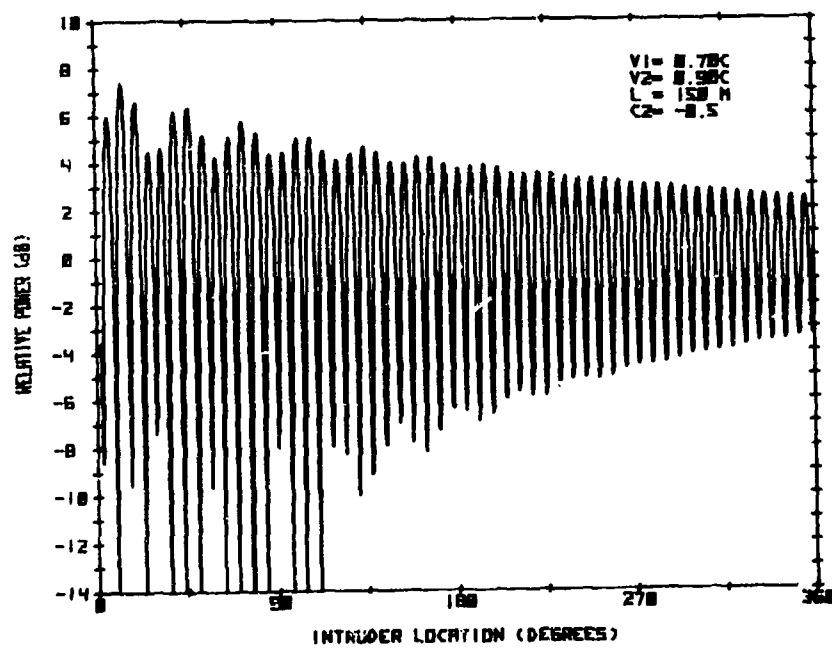


Figure 5. Received Power Variation. $|V| = |V_I|$, $\alpha_1 = 7.5 \times 10^{-3}$ neper/m, and $\alpha_2 = 3.77 \times 10^{-2}$ neper/m

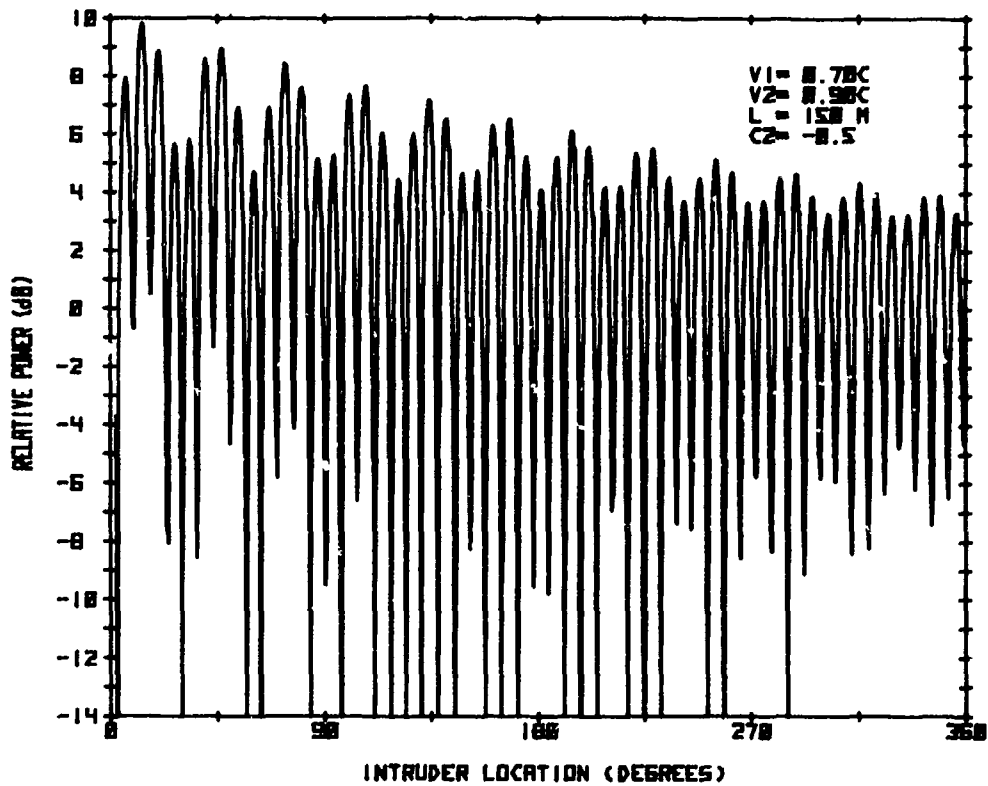


Figure 6. Received Power Variation. $1.5|V_1| = |V_I|$, $\alpha_1 = 7.5 \times 10^{-3}$ neper/m, $\alpha_2 = 1.51 \times 10^{-2}$ neper/m

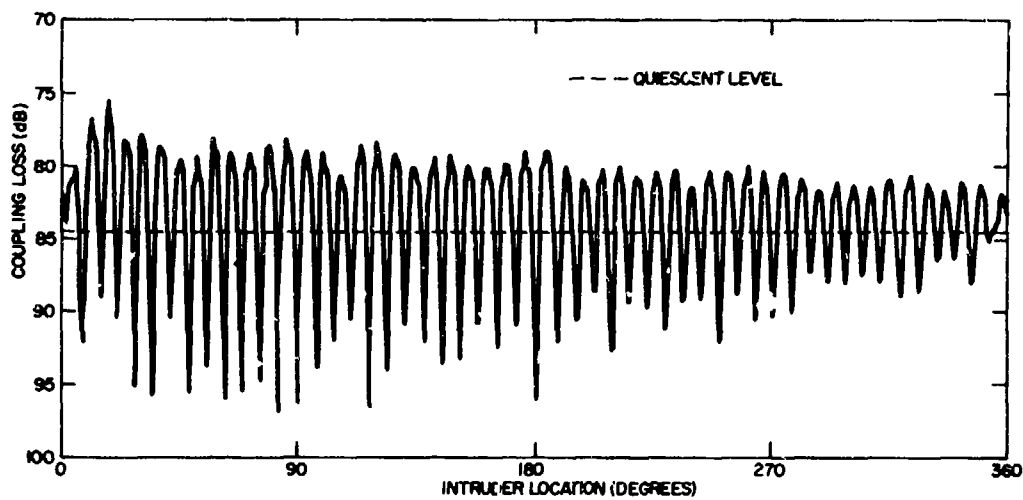


Figure 7. Measured System Response. $f = 75$ MHz, $L = 152$ m, $\alpha_1 = 8.3 \times 10^{-3}$ neper/m

scattering cross section. Comparison of the measured response with the computed curves shows an over-all agreement between the two.

2.2 Response to an Intruder for a Square Loop

The preceding analysis can be applied to a square loop, with only slight modification. From the geometry of the loop (Figure 8), it can be seen that the principal change is that the propagation factor P must now account for the change in path length from the intruder to the antenna as his position along the square varies. The new expression for V_I becomes

$$V_I = v_o A \frac{e^{i\beta_3[(D-z)^2 + D^2]^{1/2}}}{[(D-z)^2 + D^2]^{1/2}} \left\{ e^{(-\alpha_1 + j\beta_1)(z+2nD)} + C_2 e^{(-\alpha_2 + i\beta_2)(z+2nD)} \right\} \quad (8)$$

for $0 \leq z \leq 2D$ and $n = 0, 1, 2, 3$. The length of one side of the loop is $2D$, n is the index number of the side, β_3 is the free-space phase constant, and the scattered field is assumed to vary as $1/r$ with distance from the intruder. With this value of V_I , the total power at the receiving antenna is found to be proportional to

$$V_T V_T^* = B^2 + \frac{2AB|v_o|}{[(D-z)^2 + D^2]^{1/2}} \left\{ e^{-\alpha_1(z+2nD)} \cos [\phi - \beta_3[(D-z)^2 + D^2]^{1/2} - \beta_1(z+2nD) - \delta] + C_2 e^{-\alpha_2(z+2nD)} \cos [\phi - \beta_3[(D-z)^2 + D^2]^{1/2} - \beta_2(z+2nD) - \delta] \right\} + \frac{A^2|v_o|^2}{[(D-z)^2 + D^2]} \left\{ e^{-2\alpha_1(z+2nD)} + 2C_2 e^{(-\alpha_1 - \alpha_2)(z+2nD)} \cos [(\beta_2 - \beta_1)(z+2nD)] + C_2^2 e^{-2\alpha_2(z+2nD)} \right\} \quad (9)$$

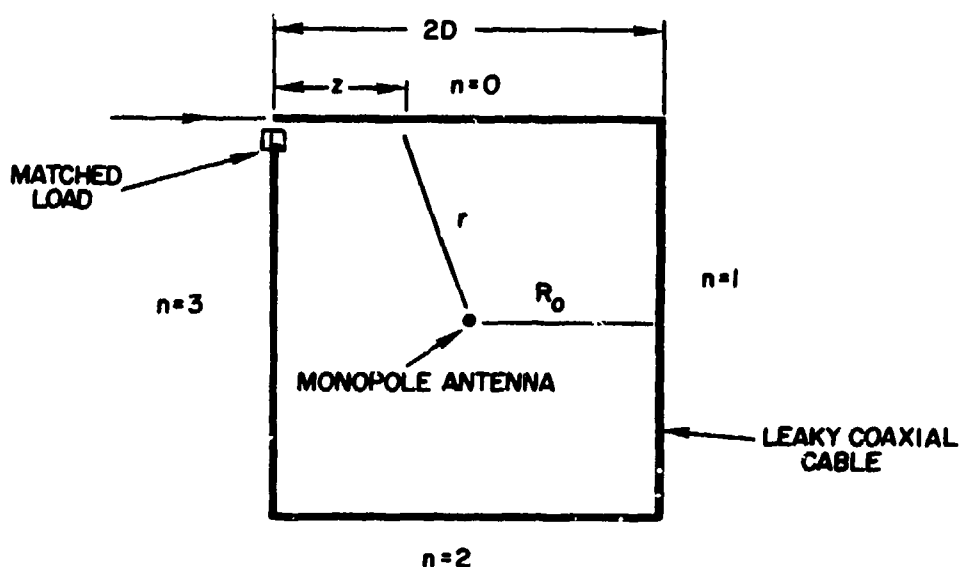


Figure 8. Sketch of Square Loop Intrusion Sensor Layout

The main feature of Eq. (9) which distinguishes it from the corresponding expression for the circular loop is contained in the cross term. Inspection shows that the effective phase of the interference term depends on the location of the intruder. A local phase constant⁸ can be obtained by differentiating the argument of the interference term. The result for the coaxial mode contribution is found to be

$$\beta = \beta_1 - \beta_3 \frac{(D - z)}{[(D - z)^2 + D^2]^{1/2}} \quad (10)$$

A graph of the second term of this function is shown in Figure 9. Inspection shows that β varies from $\beta_1 - \beta_3/\sqrt{2}$ at the beginning of a side and increases to $\beta_1 + \beta_3/\sqrt{2}$ at the end of the side. At the midpoint $\beta = \beta_1$, the value which applies to a circular loop of radius D . The steadily increasing local phase constant produces an interference pattern whose period decreases along each side. This is evident from the plot of Eq. (9) shown in Figure 10 which shows the distinctive variation in interference along each side. The over-all decrease in response is due to the attenuation of the signal. Close inspection of the response for one side, shows that the

8. Carlson, B.A. (1975) Communications Systems, An Introduction to Signals and Noise in Electrical Communications, 2nd ed., McGraw-Hill Co., New York.

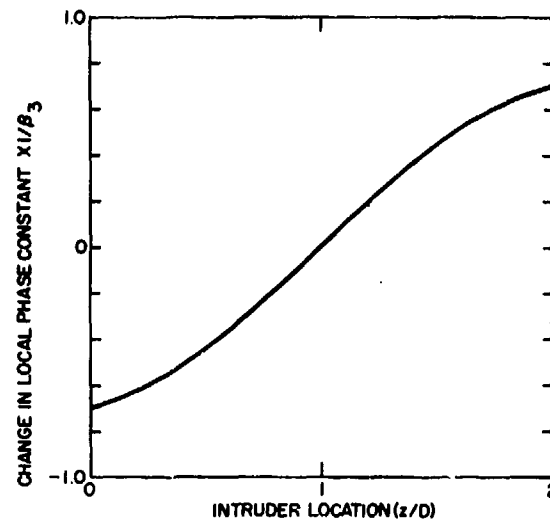


Figure 9. Graph of Change in the Local Phase Constant with Position

amplitude is greater at the midpoint than at the ends. This occurs because the $1/r$ signal loss is greater when the intruder is near the ends of the side.

The effect of reducing the relative intensity of the intruder power is shown in Figure 11 where the reduced visibility of the interference is apparent. The response shown in this figure should be compared with that observed in an experiment shown in Figure 12. The distinctive interference pattern along each side is clearly visible. It should be pointed out, however, that in the measurements the leaky cable input was at the center of the first side, while the computed patterns were based on a configuration where the input was at one corner. This difference affects only the character of the response of the first side.

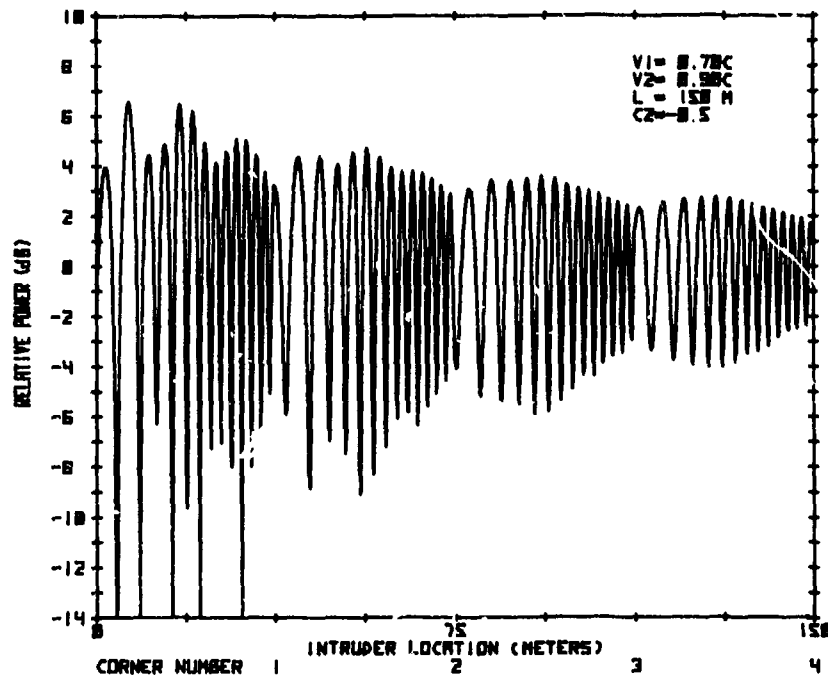


Figure 10. Variation in Received Power for Square Loop.
 $|V| = |V_I|$, $\alpha_1 = 7.5 \times 10^{-3}$ neper/m, $\alpha_2 = 3.77 \times 10^{-2}$ neper/m

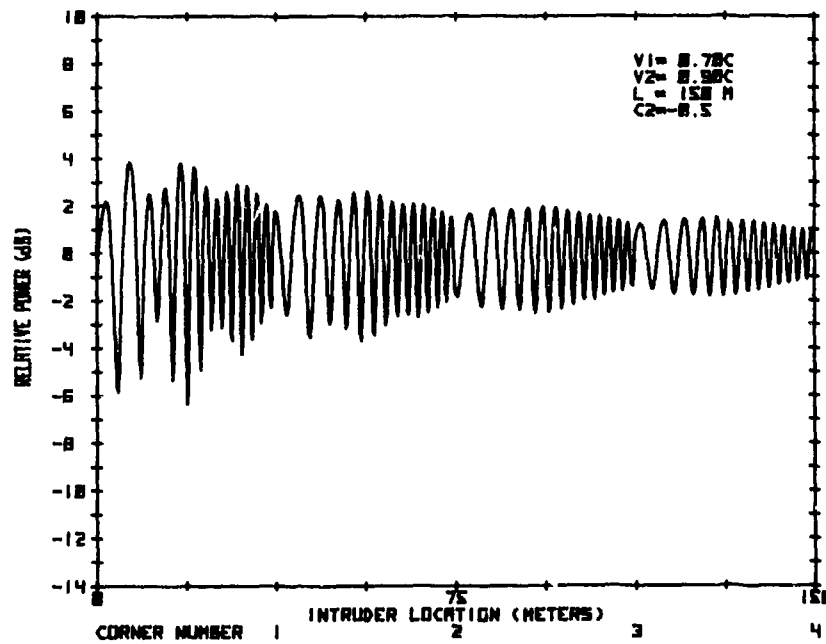


Figure 11. Variation in Received Power for Square Loop.
 $0.7|V| = |V_I|$, $\alpha_1 = 7.5 \times 10^{-3}$ neper/m, $\alpha_2 = 3.77 \times 10^{-2}$ neper/m

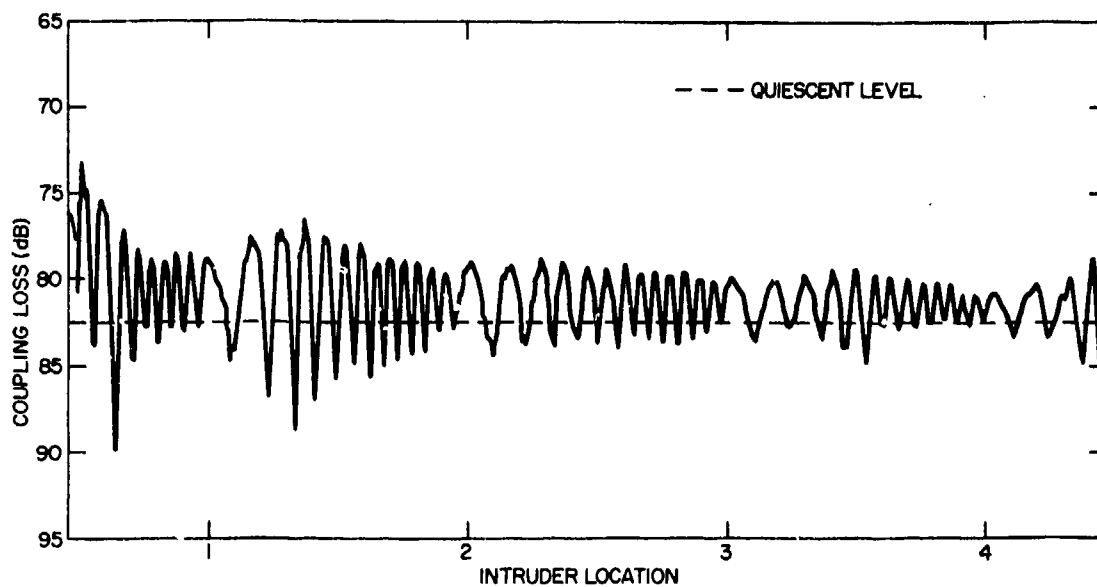


Figure 12. Measured System Response for Square Loop. $f = 75$ MHz,
 $L = 152$ m, $\alpha_1 = 8.3 \times 10^{-3}$ neper/m

3. DISCUSSION

From the previous analysis and its agreement with measurements, it is clear that the observed variation in received power is a result of the interference between the quiescent and scattered signals. The visibility of the interference depends on the relative amplitude of the two signals. Beyond this, the fine structure of the response is associated with the complex propagation constants associated with the coaxial and surface wave modes of the leaky coaxial cable. The attenuation factors produce a gradual reduction in response along the cable. The high propagation velocity of the surface wave produces the slow variations in response observed in most of the figures.

It is interesting to notice that the fields at any point along the cable sensor are principally due to the inner coaxial mode leaking out in that neighborhood. Only little of the total energy represents the contribution from the surface wave mode. This is particularly evident in Figure 5 where $\alpha_2 \gg \alpha_1$. The effect of the surface wave dies out completely over the last half of the cable.

An ideal sensor should have a uniform response along its entire perimeter. The two factors which cause the envelope of the response to vary are the attenuations of the coaxial and surface wave modes. The first produces a general reduction in the amplitude of the response with distance along the cable. The coaxial

mode attenuation factor should be small. The surface wave is responsible for the slow variations in response with position. A high surface wave attenuation factor would cause this interaction to die out rapidly, leaving only the coaxial mode field.

The response of a system using a Radiax leaky cable sensor is shown in Figure 13. For this case, $\alpha_1 = 2.3 \times 10^{-3}$ neper/m, a value significantly smaller than that associated with the CERT cable represented in the previous figures. The rapid attenuation of the surface wave and the more uniform response is evident. The Radiax cables are less lossy but much more rigid than the CERT cable. The former would be used in a permanent installation whereas the latter is appropriate in a portable system which must be deployed quickly or moved often.

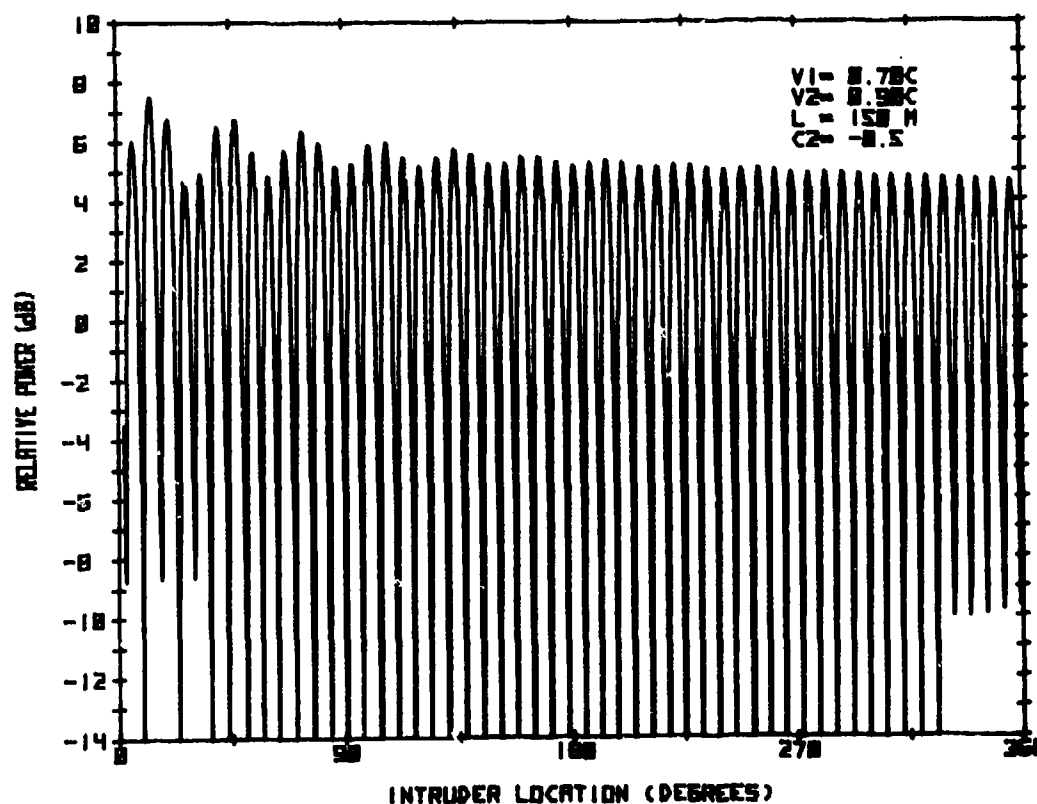


Figure 13. Variation in Received Power for Radiax Leaky Coaxial Cable. $\alpha_1 = 2.3 \times 10^{-3}$ neper/m, $\alpha_2 = 3.77 \times 10^{-2}$ neper/m, $|V| = |V_1|$

4. CONCLUSION

The previous results demonstrate the validity of the simple phenomenological theory upon which the analyses were based. The precise structure of the fields around the leaky cable and their interaction with the intruder were not known. Instead it was assumed that the principal effect of the intruder was to scatter some energy out from the fields around the leaky cable. The phase and amplitude of this scattered field were assumed proportional to the field in which the intruder was immersed. Thus the phase and amplitude of the scattered field changed as he moved around the leaky cable, giving rise to the interference which was observed. Upon these basic assumptions, it was possible to predict successfully the response of the system to an intruder.

The theory can now be used to predict performance under new conditions and to evaluate the dependence of its response on various system parameters. In particular, the effect of relative intruder size, attenuation and phase constants for the coaxial and surface wave modes, loop configuration, and the properties of the medium can be readily evaluated. The analysis can be easily extended to allow the prediction of the response to radial crossings, or to account for multiple receiving antenna.

References

1. Delogne, P. (1976) Basic mechanisms of tunnel propagation, Radio Sci. 11:295-303.
2. De Keyser, R., Delogne, P., Deryck, L., and Liegeois, R. (1978) Comparative analysis of leaky cable techniques for mine communications, Proc. Workshop on Electromagnetic Guided Waves in Mine Environments.
3. Harman, R. K., Mackay, N. A. M. (1976) GUIDAR: An intrusion detection system for perimeter protection, Proc. 1976 Carnahan Conference on Crime Countermeasures, University of Kentucky, Lexington, Ky.
4. Poirier, J. L., Karas, N. V., Antonucci, J. A., and Szczytko, M. (1977) VHF Intrusion Detection: A Technique for Parked Aircraft, RADC-TR-77-384, AD A051144.
5. Karas, N. V., Poirier, J. L., Antonucci, J. A., and Szczytko, M. (1978) A VHF Intrusion Detection Technique for Isolated Resources, RADC-TR-78-177, AD A060791.
6. Bulletin 1058A, Radiax Slotted Coaxial Cable, Andrew Corp., Orland Park, Ill.
7. Technical Memo 49, Revision No. 1, Times Wire and Cable Co., Wallingford, Connecticut.
8. Carlson, B. A. (1975) Communications Systems. An Introduction to Signals and Noise in Electrical Communications, 2nd ed., McGraw-Hill Co., New York.